

**Fixel-based Evidence of Microstructural Damage in Crossing Pathways Improves
Language Mapping in Post-stroke Aphasia**

Jie Zhang^{1,2}, Weihao Zheng³, Desheng Shang⁴, Yating Chen², Shuchang Zhong², Jing Ye², Lingling Li¹, Yamei Yu¹, Li Zhang², Ruidong Cheng², Fangping He¹, Dan Wu³, Xiangming Ye², and Benyan Luo^{1,5,*}

1 Department of Neurology & Brain Medical Center, The First Affiliated Hospital, Zhejiang University School of Medicine, Hangzhou, China

2 Rehabilitation Medicine Center & Rehabilitation Research Institute of Zhejiang Province, Zhejiang Provincial People's Hospital, Affiliated People's Hospital, Hangzhou Medical College, Hangzhou, China

3 Key Laboratory for Biomedical Engineering of Ministry of Education, College of Biomedical Engineering and Instrument Science, Zhejiang University, Hangzhou, China

4 Department of Radiology, The First Affiliated Hospital, Zhejiang University School of Medicine, Hangzhou, China

5 Collaborative Innovation Center for Brain Science, Zhejiang University School of Medicine, China

***Corresponding author:** Benyan Luo,
79 Qingchun Road, Hangzhou, 310003, China
E-mail: luobenyan@zju.edu.cn; Tel: +86-13967166677; Fax: 057187235101

Supplemental Methods:

Supplemental Method 1. Steps for calculating voxel-wise metrics

(1) Fixel-derived voxel-wise metrics:

Variables were extracted using the *fixel2voxel* command with different options (i.e., -complexity, -coord) in MRtrix3. Accordingly, the density of primary fiber population (FD1) depicts the fiber density along the principal axis, while FD2 and FD3 stand for fiber densities of secondary and tertiary populations respectively (Grazioplene et al. 2018). To compare the difference of FD along multiple crossing-fiber orientations within a voxel, complexity (CX) is calculated by:

$$CX = \frac{n}{n-1} \left(1 - \frac{\max FD_i}{\sum_{i=1}^n FD_i} \right), \text{ with } n > 1 \text{ (Riffert et al. 2014)}$$

CX ranges from 0 to 1; CX of 0 stands for only a single fiber within a voxel, while 1 represents the same fiber density along all peaks in a voxel (Riffert et al. 2014).

(2) Tensor-derived voxel-wise metrics:

Based on the pre-processed diffusion-weighted imaging (DWI) data after multiple steps of corrections, we used the *dwi2tensor* command to create the tensor model in MRtrix3. With the tensor2metric command, the MRtrix-derived tensor metrics were acquired. These subject tensor images were subsequently transformed into the common template space using the warps mentioned in the previous fixel-based analysis (FBA) steps.

Supplemental Method 2. Defining the tracts of interest (TOIs)

Fiber bundles of interest were extracted individually using the regions-of-interest combinations from the whole-brain template tractogram. To choose TOIs, a standardized tracking protocol from a novel cross-species tractography (XTRACT) toolbox was utilized (Warrington et al. 2020). The TOI protocol of XTRACT provides the unique combinations of inclusion and exclusion regions of interest (ROIs) for 42 white matter tracts. Among them, we selected the tracts in the dorsal and ventral streams as TOIs of this study, including the superior longitudinal fasciculus (SLF) III, arcuate fasciculus (AF), inferior fronto-occipital fasciculus (IFOF), uncinata fasciculus (UF), inferior longitudinal fasciculus (ILF), middle longitudinal fasciculus (MdLF), and frontal aslant tract. Here, we did not continue the step of probabilistic tractography from XTRACT toolbox and merely utilized the combinations of inclusion and exclusion ROIs for TOIs in its protocol. These ROIs, defined in standard space (MNI152 for human brain), were warped into the template space provided by MRtrix3.

The tracts in the template space obtained by template-based tractography were binarized into masks of TOIs. Mean values of TOI for voxel-wise metrics could be extracted by these binarized masks. Regarding fixel-wise metrics, we projected values from three-dimensional voxel-level masks into the fixels underlying each voxel using the *voxel2fixel* command, and then calculated the mean values within the fixel masks of

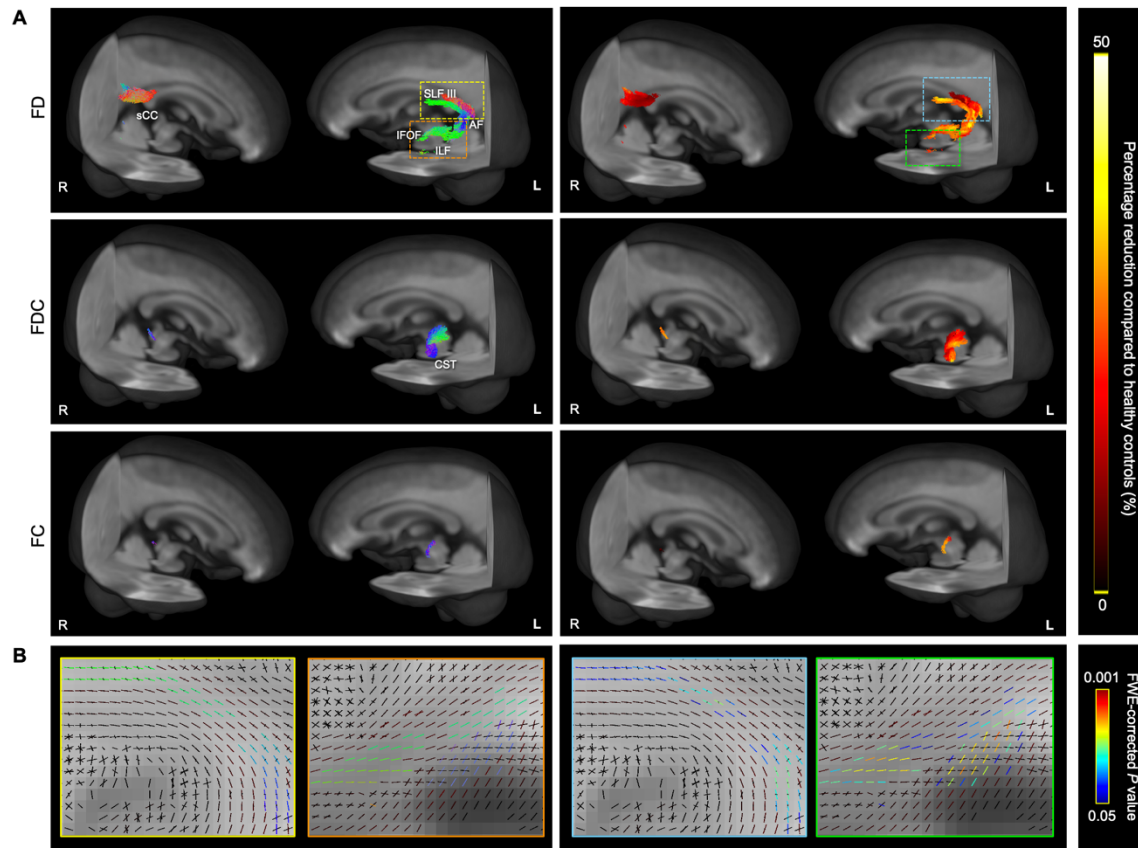
interest.

For two-group comparison of tract-wise metrics, the number of selected tract is 7 (the left SLF III, AF, front aslant tract, IFOF, ILF, UF, MdLF), while the number of evaluated metrics is 4 (FD, FDC, FC, FA), therefore Bonferroni-adjusted p is $0.05/(4*7)=0.002$. For correlation of tract-wise metrics, we chose metrics with significant 2-group difference: mean FD of the left SLF III, AF, IFOF, and UF, and mean FA of the left SLF III, AF, IFOF, and MdLF; therefore, Bonferroni-adjusted p for tract-wise correlation is $0.05/8=0.006$.

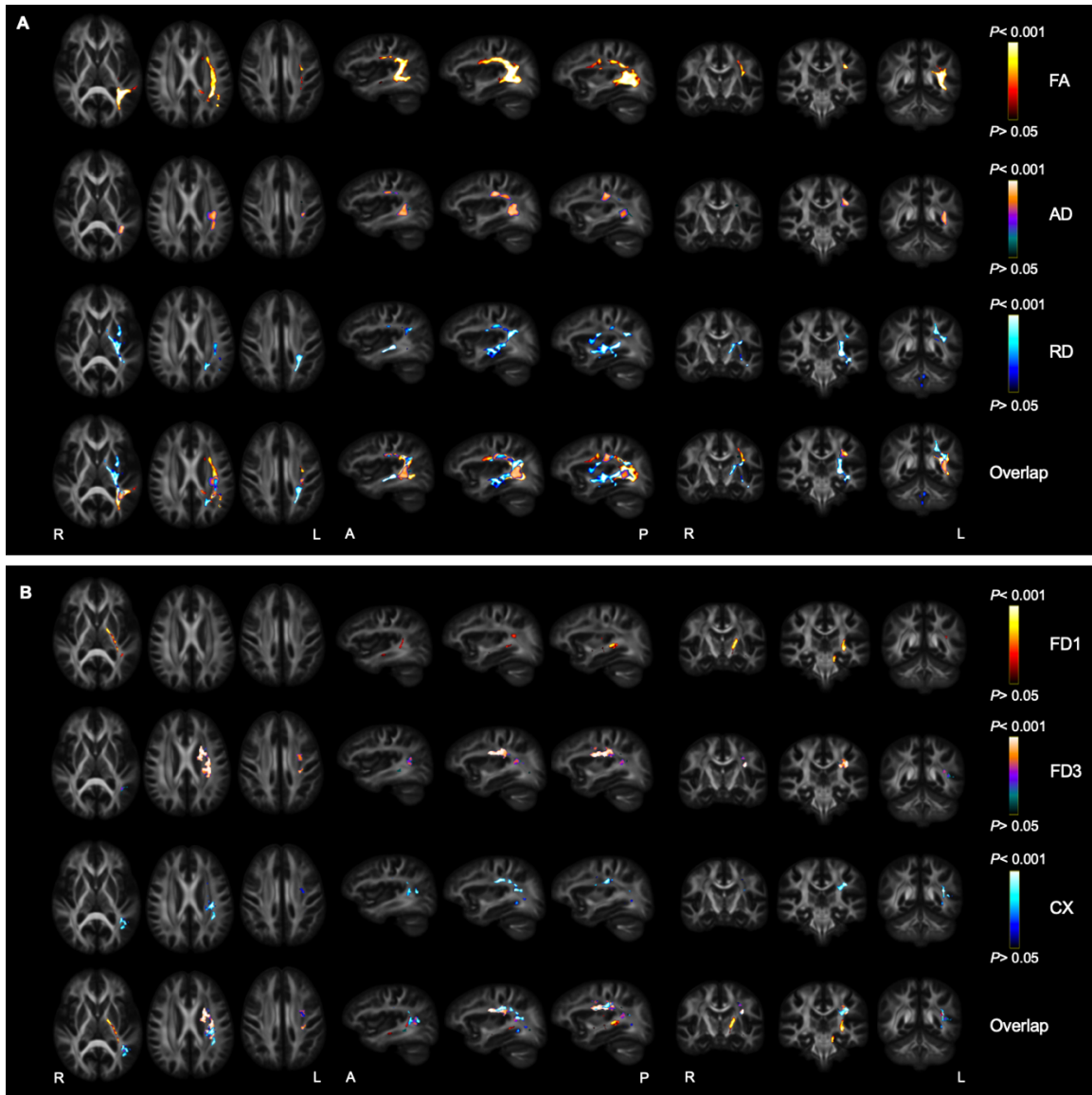
Supplemental Table:**Supplemental Table 1. Detailed language score percentage of Aphasia Battery of Chinese (ABC) in aphasic patients (n = 29)**

| Language Domain | Subdomain | Mean (%) | Median (%) | Quartile (%) |
|------------------------|---------------------|-----------------|-------------------|---------------------|
| Comprehension | Total | 44.6 | 31.7 | (22.6, 69.8) |
| | Word-level | 50.2 | 46.7 | (23.9, 87.8) |
| | Sentence-level | 41.1 | 32.1 | (18.6, 62.1) |
| Repetition | Total | 32.4 | 20.0 | (0.5, 60.5) |
| | Word-level | 50.1 | 41.7 | (2.1, 100.0) |
| | Sentence-level | 26.9 | 5.9 | (0.0, 48.7) |
| Naming | Total | 25.2 | 3.2 | (0.0, 48.4) |
| | Picture naming | 26.4 | 5.0 | (0.0, 55.0) |
| | Color naming | 25.6 | 0.0 | (0.0, 58.3) |
| | Responsive naming | 22.8 | 0.0 | (0.0, 50.0) |
| Reading | Total | 28.2 | 9.2 | (4.6, 54.6) |
| | Word-level | 34.6 | 15.0 | (6.7, 63.3) |
| | Sentence-level | 21.8 | 5.0 | (0.0, 44.2) |
| Writing | Total | 16.8 | 0.5 | (0.0, 44.3) |
| | Dictation | 15.4 | 0.0 | (0.0, 30.0) |
| | Copying | 51.7 | 80.0 | (0.0, 100.0) |
| | Spontaneous writing | 20.9 | 0.0 | (0.0, 54.5) |
| Spontaneous Speech | - | 36.7 | 34.1 | (28.9, 46.3) |
| Aphasia Quotient (AQ) | - | 40.3 | 30.6 | (21.5, 62.0) |

Supplemental Figures:



Supplemental Fig. 1. Significant fixel-wise reductions in post-stroke aphasia compared to controls, adjusted by an additional covariate motor dysfunction degree. Images are shown on the population-template, displayed as three-dimensional streamlines cropped from the template tractogram (family-wise error-corrected P-value < 0.05). **A**, Tract-specific streamlines represent mapped fixels with significantly reduced fiber density (FD), fiber density and bundle cross-section (FDC), and fiber-bundle cross-section (FC) values. **B**, Enlarged crossing-fiber areas with significant fixels of FD reductions. Left panels: colors are encoded by fixel direction (green: anterior-posterior, blue: superior-inferior, red: left-right); right panels: streamline points are colored by percentage reductions of fixel-wise metrics compared to the control group, and zoomed fixels are colored by family-wise error-corrected P-value of group-wise comparisons. AF = arcuate fasciculus; CST= corticospinal tract; IFOF = inferior fronto-occipital fasciculus; ILF = inferior longitudinal fasciculus; sCC = splenium of the corpus callosum; SLF = superior longitudinal fasciculus.



Supplemental Fig. 2. Group differences in the fixel- and tensor-derived voxel-based analyses between post-stroke aphasia patients and healthy controls. A, Tensor-derived metrics with significant alterations are colored according to P-values. Voxels show reduced FA (yellow), reduced axial diffusivity (purple), and increased radial diffusivity (blue) in post-stroke aphasic patients compared to healthy controls, as well as their overlap. **B,** Fixel-derived metrics with significant alterations are colored according to P-values. Voxels show reduced FD1 (yellow), increased FD3 (purple), and increased complexity (blue) in post-stroke aphasic patients compared to healthy controls, as well as their overlap. AD = axial diffusivity; CX = complexity; RD = radial diffusivity.

Supplemental References

- Grazioplene, R. G., Bearden, C. E., Subotnik, K. L., Ventura, J., Haut, K., Nuechterlein, K. H., et al., 2018. Connectivity-enhanced diffusion analysis reveals white matter density disruptions in first episode and chronic schizophrenia. *Neuroimage Clin.* 18, 608-616. <https://doi.org/10.1016/j.nicl.2018.02.015>.
- Riffert, T. W., Schreiber, J., Anwender, A., & Knosche, T. R., 2014. Beyond fractional anisotropy: extraction of bundle-specific structural metrics from crossing fiber models. *Neuroimage.* 100, 176-191. <https://doi.org/10.1016/j.neuroimage.2014.06.015>.
- Warrington, S., Bryant, K. L., Khrapitchev, A. A., Sallet, J., Charquero-Ballester, M., Douaud, G., et al., 2020. XTRACT - Standardised protocols for automated tractography in the human and macaque brain. *Neuroimage.* 217, 116923. <https://doi.org/10.1016/j.neuroimage.2020.116923>.